plasma process group

Simple Ion Beam Solutions

Ion Beam Sputtering

B. Buchholtz
Plasma Process Group, 7330 Greendale Rd., Windsor, CO, 80550

In this paper, the fundamentals of ion beam sputtering as it is used to deposit precise layers will be discussed. This paper has been outlined to start with the basics of ion beam operation, followed by the physics of sputtering, and finally the deposition characteristics. Even though ion beam sputtering is used in the optics industry to produce low loss optics and the emphasis in this article will pertain to the deposition of dielectric materials, it is hoped the subject matter within will also be useful for other applications.

Introduction

Ion beam thrusters, or broad-beam ion source technology was initially developed in the 1960's by the electric propulsion group within the National Aeronautics and Space Administration [1,2]. Ion beam sources are attractive for space propulsion due to their high specific impulse. However, for terrestrial applications ion beam sources can be used for sputtering material, ion etching, ion plating and various other techniques for material modification and enhancement. The emphasis of this article will pertain to the physics of sputtering using an ion beam.

First, a quick examination of ion beam sources and their operation will be covered. Next, a simple ion beam deposition layout will be discussed and terms defined. Concepts such as sputter yield, etch rate and deposition rate will be introduced and examples are provided. Finally, common parameters found in ion beam sputtering and their descriptions are compiled.

Ion Beam Sources and Operation

Ion beam sources are usually classified by the initial beam diameter at the source and by the type of discharge used to create the ions. Commercially available ion beam sources are typically cylindrical with diameters that range from 3 to 30 cm but rectangular models are also available. The two types of discharges discussed herein are direct current (DC) and radio frequency (RF). Sources which utilize either

a filament cathode or hollow cathode are referred to as DC type and those which utilize an induction coil are RF type.

Illustrated in Figure 1 is a cross-sectional schematic of an RF ion beam source and the electrical connections. An ion beam source is operated by ionizing a feed gas and then extracting these ions at a controlled energy. For sputtering applications, the feed gas is typically high purity Argon (99.999%). However, other noble gases such as Krypton and Xenon can be used. Gasses such as Oxygen, Nitrogen, and Methane can be used for application specific material modifications. The gas flow rate is selected according to the size of source and pumping speed of the high vacuum environment. Flow rate is measured in standard cubic centimeters per minute (sccm) and a typical background pressure during operation is about $5x10^{-4}$ mbar.

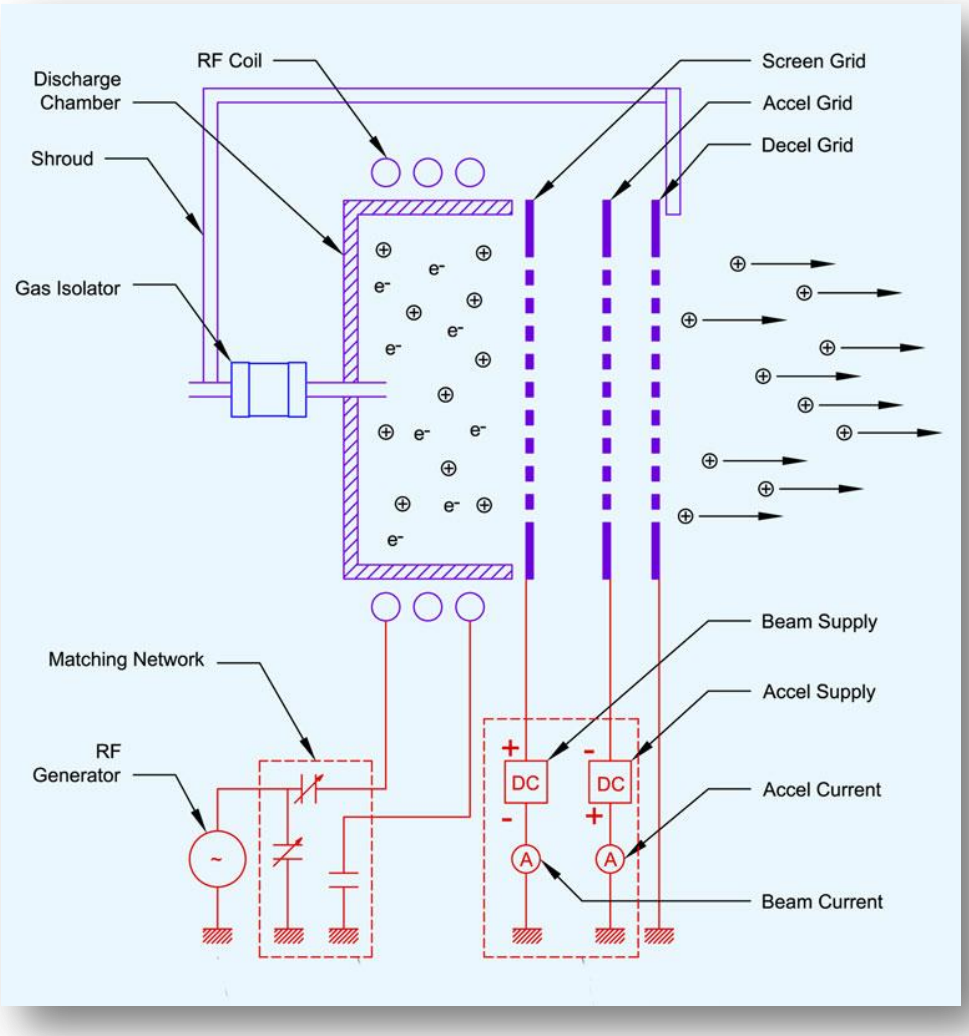

Figure 1. Schematic of an RF ion beam source with IBEAM power supply.

Argon is introduced into the discharge chamber through a gas isolator. The gas isolator allows flow of argon while maintaining electrical isolation between the discharge chamber and shroud. The shroud provides mechanical support and in some cases cooling. The discharge chamber is fabricated from a dielectric such as quartz or alumina. This allows the field generated by the RF coil to penetrate the discharge chamber and ionize the argon. The plasma density, or number of ions per unit volume, inside the discharge chamber is proportional to the applied RF power [3]. The RF circuit requires a matching network to accommodate the various loads produced by the plasma.

Ions from the discharge chamber plasma are extracted using a series of electrostatic grids, or ion optics, that have many precisely aligned apertures, or holes. An example of a grid assembly with over 3600 holes is shown in Figure 2. Aperture size and spacing are design dependent, however, both are typically on the order of 1 mm. Grids are typically fabricated from either Molybdenum or Graphite. The screen grid is biased positive with respect to ground potential using a DC supply as illustrated in Figure 1. The accelerator grid is biased negative with respect to ground and the decelerator grid (if used) is electrically connected to ground.

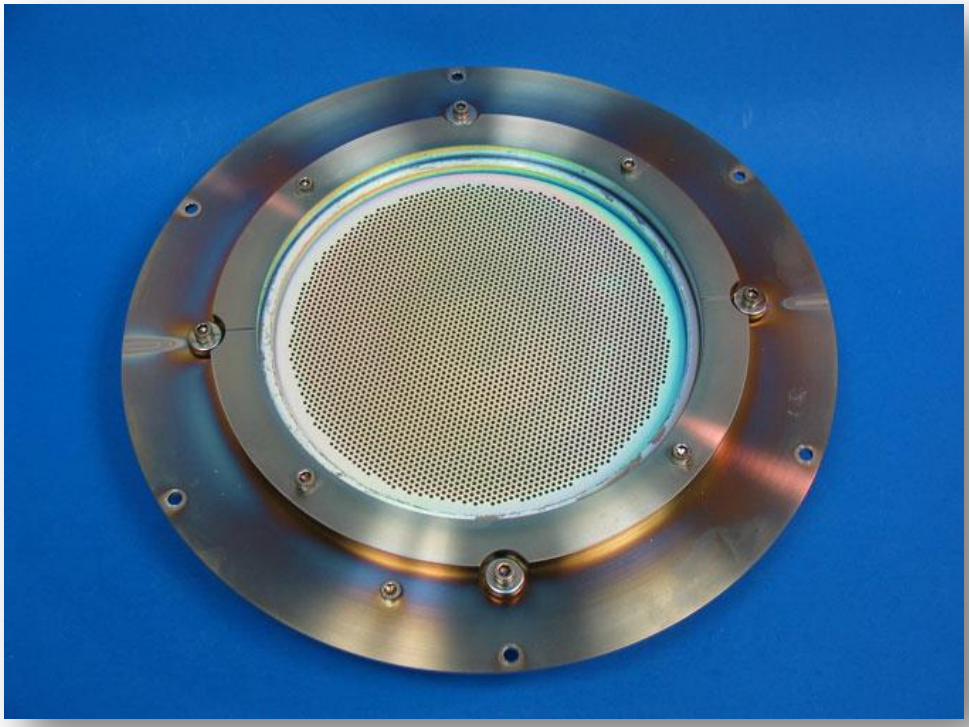

Figure 2. Grids for a 16 cm RF source.

In order to understand how ions are extracted, plotted in Figure 3 is a schematic of the electric field potential variation through a cross section of one hole within the grid assembly. With the plasma inside the discharge chamber biased positive, ions are attracted to the negative accelerator grid. As ions accelerate towards the accelerator grid, their velocity increases. Due to the established electric field, the ions travel through the individual apertures, form beamlets and leave the source. Ion energy is determined by the electrostatic potential of the screen grid, or beam voltage. The total number of ions leaving the source is defined as the beam current. Beam current is measured using an ammeter on the beam supply (Figure 1), and for RF sources, is proportional to the applied RF power.

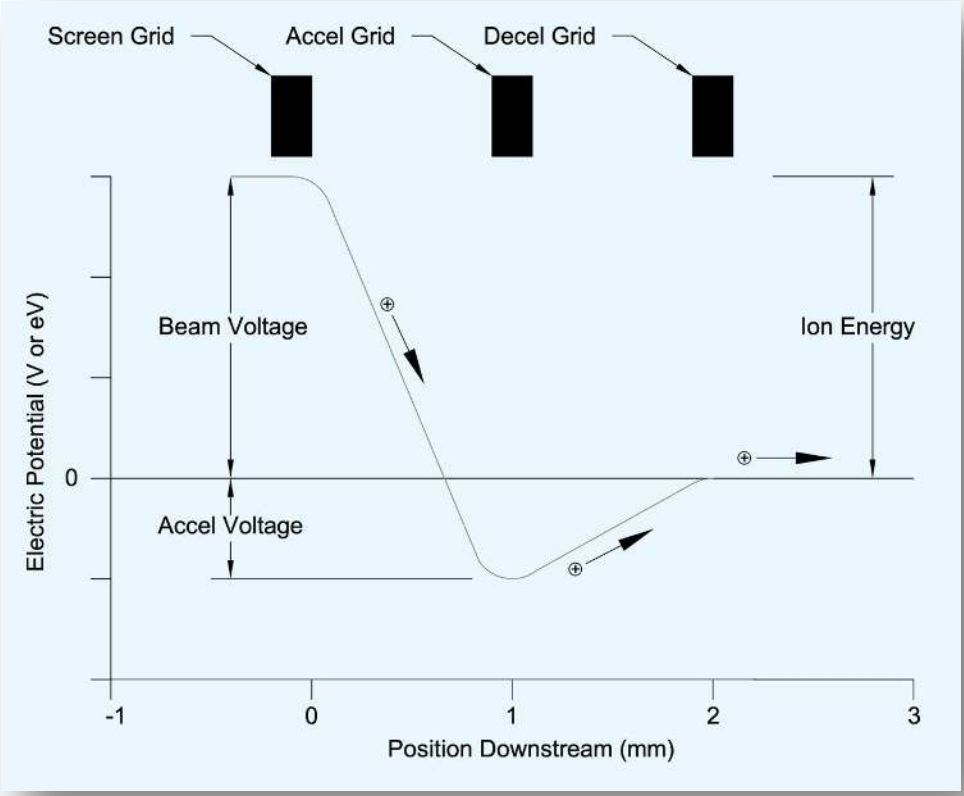

Figure 3. Electrostatic potential gradient through ion optics.

The accelerator grid design and its electrical potential will determine the degree of beamlet collimation [4]. The collimation, or focus, of individual beamlets is typically proportional to the accelerator voltage. Individual beamlets can be spread or flared by increasing accelerator voltage. However, care must be taken as too high of an accelerator voltage will result in direct ion impingement on the decelerator grid. The current measured to the accelerator grid is primarily a result of

charge-exchange reactions between the high velocity ions and neutral feed gas in the vicinity of the grid apertures [5]. For properly aligned grids and reasonable operating conditions, the accelerator current is typically less than 10% of the beam current.

The decelerator grid design will also influence the beamlet collimation and is not required for the ion beam source to operate. However, for sputter deposition applications, the decelerator grid is primarily used as a shield to capture sputtered material and protect the accelerator grid from becoming coated. As a result, the beamlet trajectories are more stable over time.

The final component for an ion beam source is a neutralizer as depicted in Figure 4. The purpose of the neutralizer is to emit electrons into the environment downstream from the ion beam source. In this fashion, the electrons prevent charge build up on downstream surfaces and provide *space-charge neutralization* of the positive ion beam [6]. Typically, neutralizers emit more electrons than ions emitted from the source. The total number of emitted electrons is defined as the emission current and is typically 150 to 200% of the beam current. Different types of neutralizers include RF, hot-filament, and hollow cathode.

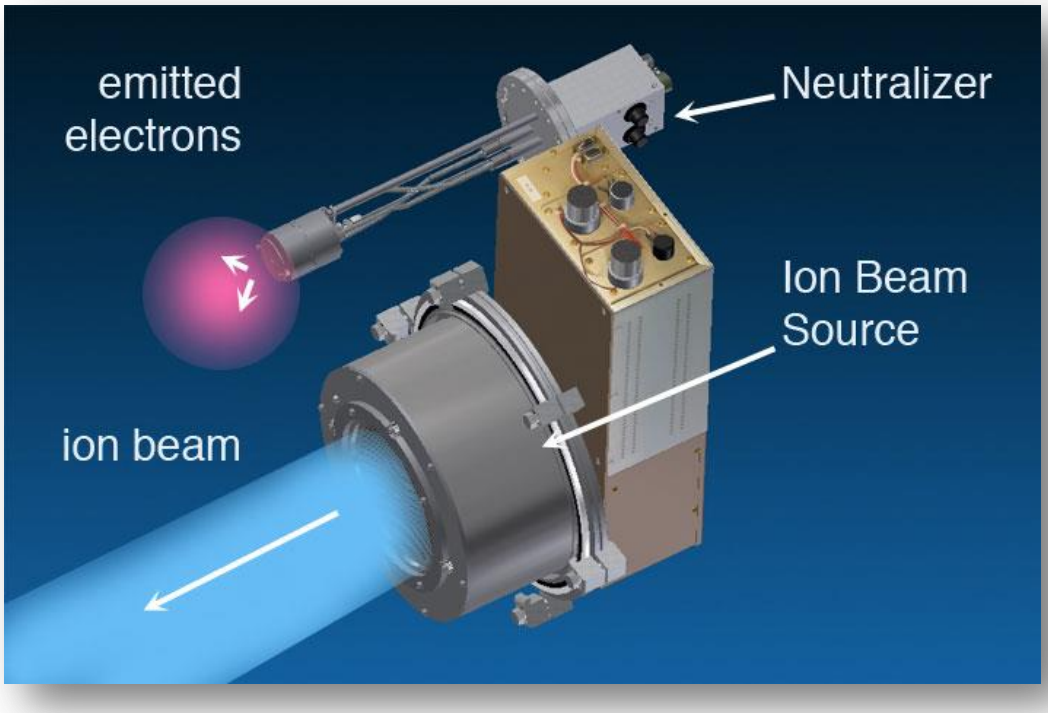

Figure 4. Ion beam source with neutralizer.

Ion Beam Sputter Deposition Layout

In a basic arrangement, an ion beam sputtering (IBS) system consists of an ion beam source, target, and substrate enclosed in a vacuum chamber as depicted in Figure 5. The ion beam source is directed at the target at an off-normal angle. Collisions between the ions and the target will produce sputtered atoms from the target. Target material choice is determined by the coating required on the substrates. Substrates are adjacent to the target and in close proximity to capture the sputtered material ejected. If a second ion beam source is used, it is referred to as an assist beam and the system becomes an ion beam assisted deposition (IBAD) platform.

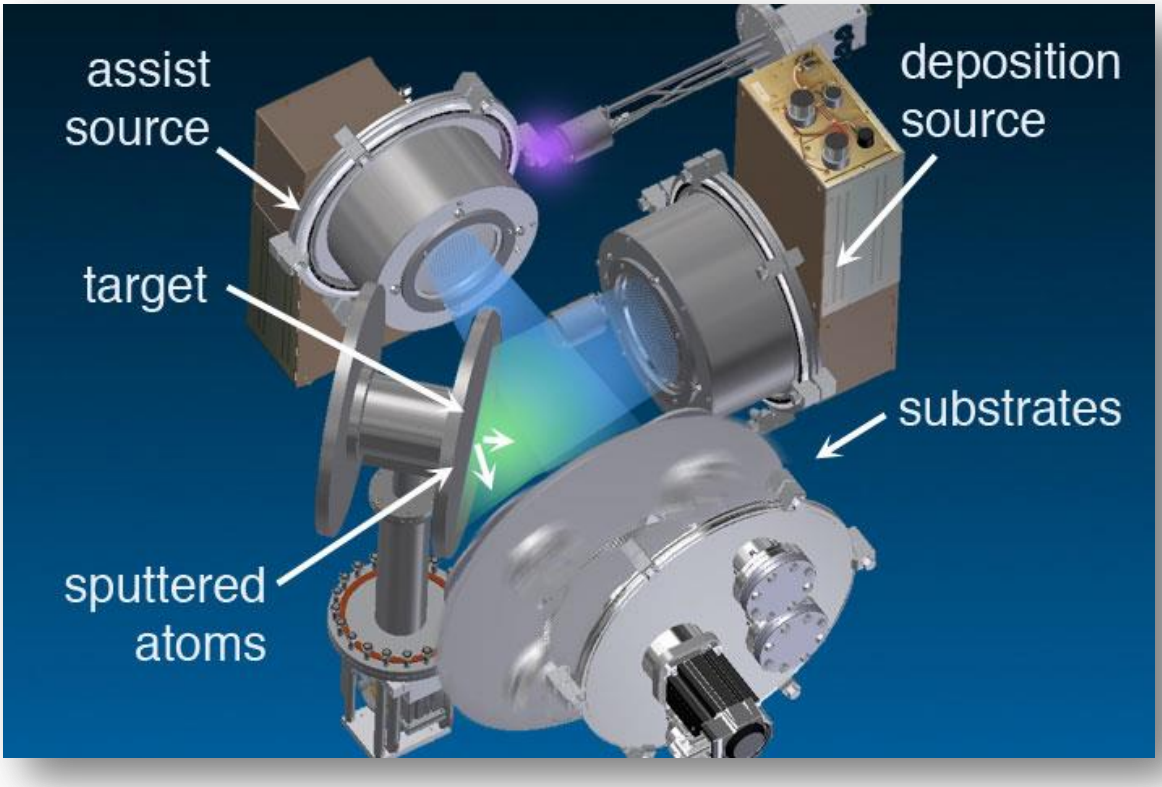

Figure 5. Ion beam sputtering (IBS) system schematic.

Sputtering target material is a momentum transfer process where target atoms are ejected due to collisions from incident ions [7,8]. The number of ejected atoms per incident ion is referred to as the sputter yield (S_y). Sputter yield is primarily a function of ion energy (i.e. both mass and velocity), angle of impact, and target material.

Sputter yield data for various ion-target combinations have been tabulated for a variety of conditions [9,10]. In addition, numerical simulations, such as SRIM, have

been developed to estimate S_y for application specific investigations [11]. Presented in Table 1 are typical sputter yield data for various materials as calculated using SRIM. The estimated S_y is determined for Argon ions with energies of 500 and 1000 eV striking the target at an angle of incidence of 0°, or normal to the target. It is important to note that a doubling of the ion energy does not necessary mean S_y has doubled.

Table 1. Sputter Yield (S_y) for materials at normal incidence (0°).

MATERIAL	NAME	S_y (atoms/ion) 500 eV Ar ion	S_y (atoms/ion) 1000 eV Ar ion
Al	Aluminum	0.66	1.08
Au	Gold	2.46	3.92
C	Carbon	0.12	0.26
Fe	Iron	1.51	2.31
Si	Silicon	0.47	0.77

Sputter yield is also dependent upon the angle of incidence of the ions striking the target. To illustrate this, the variation of S_y as calculated using SRIM for Aluminum and Tantalum sputtered by Argon ions at different target angles is plotted in Figure 6. The calculated data are considered typical examples of sputter yield variation and show a maximum yield for target angles between 60 and 75°. It is also worth noting that the sputter yield increases 5 fold for aluminum and only slightly for tantalum as the incidence angle was increased.

For sputtering applications, the most significant ion beam source operating parameters are *ion specie*, *beam voltage*, and *beam current*. A simple IBS system will use Ar for the ion specie. Gases such as O_2 and N_2 can be used or mixed with Ar for reactive sputtering. Reactive sputtering is the process of forming compounds such as oxides or nitrides. Reactive sputtering can also be performed by placing an additional gas line adjacent to the target. For example, to form the oxide Ta_2O_5, a metal Ta target is sputtered with an Ar ion beam while exposed to an O_2 gas line adjacent to the target.

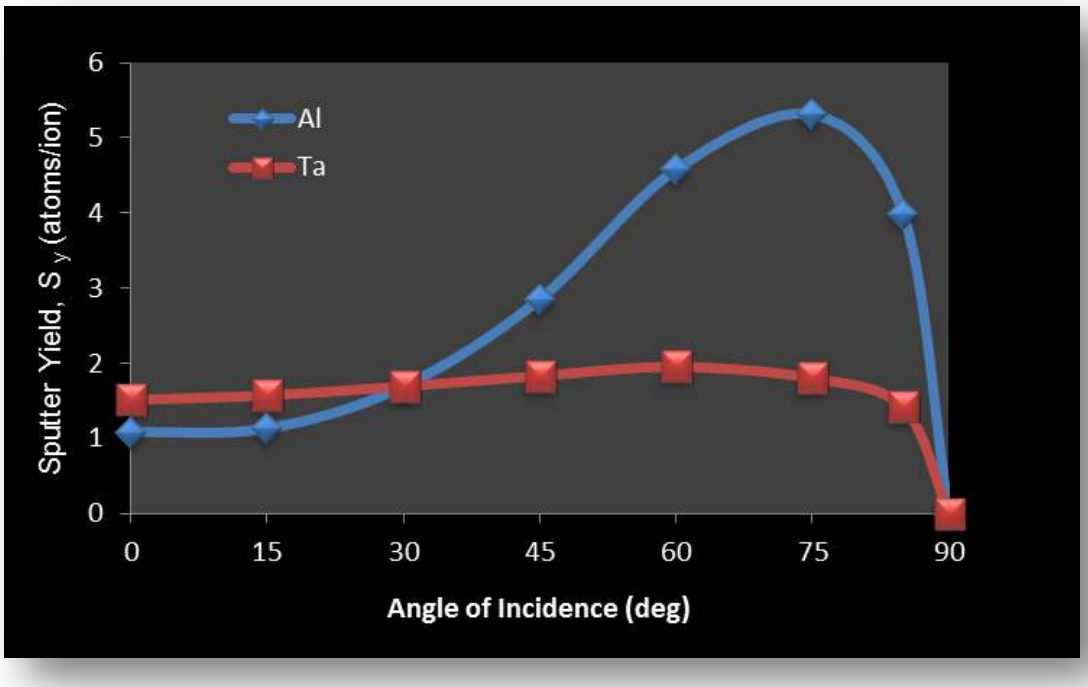

Figure 6. Variation of sputter yield with incident angle.

With ion beam sources, the beam voltage and current are independently controlled. The applied beam voltage in electron volts (eV) is the energy of the ions in the beam. Also, to first order, the beam current will be the number of ions arriving at the target. However, with consideration for source-to-target geometry and downstream environment, a measurement of the incident ion flux is more accurate. Incident ion flux to the target is measured by sweeping a Faraday probe through the beam at the target location. This type of measurement is also referred to as a *beam profile*.

A typical beam profile for an 8 cm DC source with graphite grids is plotted in Figure 7. With the source centerline at radial position of 0 cm, these data represent a cross-section of the ion beam at a location 20 cm downstream. The incident ion flux, or current density (j), increases to a maximum of about 2.5 mA/cm^2 and the total beam envelope range is from -10 to 10 cm. Two important aspects of this data are realized. First, the ion beam diameter has increased from the initial diameter of 8 cm at the source to the profile plotted in Figure 7. Second, for these given beam conditions, a target diameter of 20 cm should be selected so beam overspray is minimized.

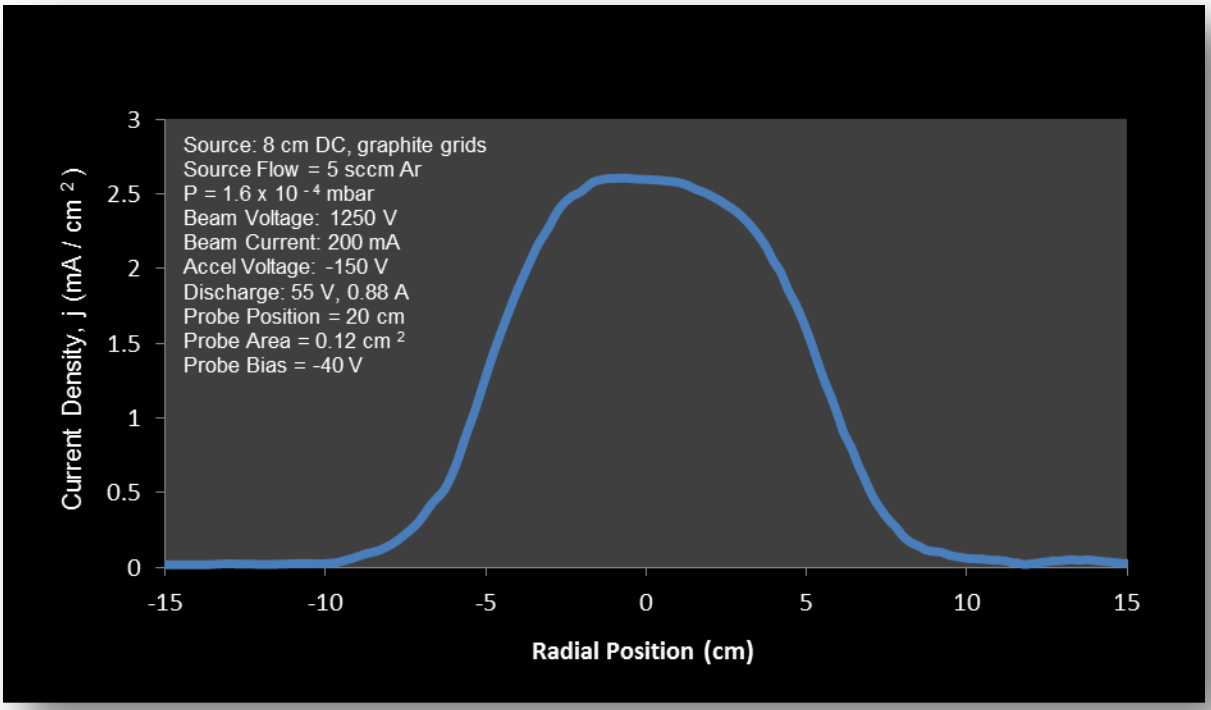

Figure 7. Current density variation with radial position.

Once beam profile data are obtained, the *etch rate* (E_r) of a target exposed to an ion beam can be estimated [7,15]. Equation 1 describes the material removal in Å/min due to the incident ion flux. For this equation, current density (j) is in mA/cm^2, target molecular weight (M_w) in g/mol and target density (ρ) is in g/cm^3. A unit correction factor of 62.29 is also required.

$$E_r = \left(62.29 \frac{\text{Å} \cdot mol}{mA \cdot \min \cdot cm}\right) \cdot \frac{j \cdot S_y \cdot M_W}{\rho} \quad \text{[Å/min]} \quad (1)$$

Presented in Table 2 are calculated etch rates for common target materials and compounds. These rates are for Argon ions with energies of 500 and 1000 eV and current density of 1 mA/cm^2. The rates were estimated by using sputter yield data from SRIM and Equation 1. The etch rate will scale with current density and can be used to determine target life.

Table 2. Etch rate estimates at normal incidence (0°) and 1 mA/cm^2 for Ar ions.

Material	Name	S_y (atoms/ion) 500 eV Ar^+	S_y (atoms/ion) 1000 eV Ar^+	M_W (g/mol)	ρ (g/cm^3)	E_r (Å/min) 500 eV Ar^+	E_R (Å/min) 1000 eV Ar^+
Ag	Silver	2.54	3.76	108	10.5	1630	2410
Al	Aluminum	0.66	1.08	27	2.7	410	673
Au	Gold	2.46	3.92	197	19.3	1560	2490
Be	Beryllium	0.31	0.51	9	1.85	92	153
Bi	Bismuth	1.85	2.71	209	9.8	2460	3600
C	Carbon	0.12	0.26	12	2.25	39	86
Co	Cobalt	1.84	2.78	58.9	8.9	759	1150
Cr	Cromium	1.41	2.07	52	7.2	634	931
Cu	Copper	2.46	3.86	63.5	8.9	1090	1720
Fe	Iron	1.51	2.31	55.8	7.87	667	1020
Ge	Germanium	1.31	1.89	72.6	5.35	1110	1600
Hf	Hafnium	1.08	1.61	179	13.3	903	1350
Ir	Iridium	1.57	2.65	192	22.4	839	1420
Mg	Magnesium	1.01	1.47	24.3	1.74	879	1280
Mn	Manganese	2.30	3.39	54.9	7.43	1060	1560
Mo	Molybdenum	1.05	1.61	95.9	10.2	615	943
Nb	Niobium	0.79	1.20	92.9	8.57	533	810
Ni	Nickel	1.93	2.96	58.7	8.9	793	1220
Pd	Palladium	2.38	3.67	106	12	1320	2030
Pt	Platinum	1.69	2.74	195	21.5	955	1550
Sb	Antimony	1.75	2.51	122	6.68	1990	2850
Si	Silicon	0.47	0.77	28.1	2.32	356	582
Sn	Tin	1.60	2.38	119	7.28	1630	2420
Ta	Tantalum	0.97	1.51	181	16.6	661	1030
Th	Thorium	0.77	1.20	232	11.7	951	1480
Ti	Titanium	0.65	0.97	47.9	4.52	429	640
V	Vanadium	0.69	1.07	50.9	5.96	367	569
W	Tungsten	1.03	1.63	184	19.4	608	963
Y	Yittrium	0.90	1.32	88.9	4.47	1110	1640
Zr	Zirconium	0.86	1.21	91.2	6.49	752	1060
Al_2O_3	Alumina	0.60	0.95	102	3.97	960	1530
Si_3N_4	Silicon Nitride	0.47	0.77	140	3.44	1200	1970
SiO_2	Quartz	0.47	0.72	60	2.32	754	1160
Ta_2O_5	Ta - Pentoxide	1.38	2.03	442	8.2	4640	6800
YBCuO	Superconductor	0.89	1.25	666	6.54	5640	7940
Az-111	Photoresist	0.09	0.15	100	0.92	587	1030
Kapton	Polyimide Film	0.05	0.11	979	1.42	1950	4550

The material ejected from the target is referred to as emitted flux. The emitted flux will have its own energy and trajectory distributions. The energy of the sputtered material is dependent upon the details of the ion-target collisions but for the examples in Table 2 the average energy will vary from 3 to 60 eV [11]. The emission flux trajectory distribution is described in terms of an angular distribution relative to the target normal. For the ideal target, the distribution is dependent upon the cosine of the angle from normal [7]. However, typical sputter yield measurements indicate the distribution has a different structure [12]. Theory and experiment may not agree due to the simplified nature of a cosine distribution. It is important to note factors such as size and shape of the ion beam, target surface roughness, and the distance from the target that the emission flux is measured play a role with the results obtained.

The substrate placed in the emission flux, or deposition plume, downstream from the target becomes coated. If reactive gases are used, compounds such as oxides are deposited. The sputtered material deposited onto the substrate will have a deposition rate, D_r. An expression for D_r which shows how the deposition rate is related to the sputter yield (S_y), current density (j) at the target, and target-to-substrate distance (d) is presented in Equation 2. The integration is performed as each unit area on the target (dA) has a contribution to the overall deposition rate. More complete descriptions of the deposition rate have been developed and are presented elsewhere [7]. For a properly designed IBS system typical deposition rates are about 2 Å/s.

$$D_r \sim \int \frac{S_y \cdot j}{d^2} dA \qquad (2)$$

Substrate motion is performed to even out the deposition, or provide a more uniform coating. As the substrate is manipulated through the deposition plume, the uneven distribution of the sputtered target material is integrated to form a more uniform coating on the substrate. Different strategies for substrate manipulation include simple rotation or planetary motion. The uniformity of a deposited coating is described by Equation 3, where t_{MAX} and t_{MIN} are the maximum and minimum coating physical thickness for a given coated area, respectively.

$$Uniformity = 100 \cdot \left(\frac{t_{MAX} - t_{MIN}}{t_{MAX} + t_{MIN}} \right) \ [\pm\%] \qquad (3)$$

There are several different methods used to measure coating thickness and determine the uniformity. The preferred method is specific to the application. Presented in Table 3 are various applications and some of the methods used to determine coating uniformity. It is recommended the uniformity for any IBS system should be calibrated at the same conditions as the final product. Run-to-run variation of the uniformity for an automated and properly maintained IBS system is on the order of 0.1%.

Table 3. Methods for determining coating uniformity.

APPLICATION	METHOD	COMMENTS
Metal Coatings	Witness piece with markings that are removed. Step-profiler used to measure thickness.	Time consuming. Does not determine optical properties.
Optical Coatings	Witness piece coated with a single layer optical film. Ellipsometer or spectrophotometer used.	Optical data are curve-fit to model. Optical constants determined.
Optical Devices	Witness piece coated with a simple Fabry-Perot type filter [13]. Optical measurement of center wavelength.	Result pertains to cavity material only.
Precision Optical Devices	Witness piece coated with a 2-peak filter [14]. Optical measurement of center wavelength for both peaks.	Time consuming.

Termination of deposition is performed by turning the beam supply off and is on the order of milliseconds. This allows for very accurate layer termination useful for depositing precise multilayer optical coatings.

Application Specific Considerations

An IBS system allows for independent control of many variables. The level of control offered by IBS is unique compared to other types of thin film deposition techniques. This makes IBS an ideal research tool for ion-target and thin film growth investigations. Below are guidelines for selection of the variables depending upon the requirements specific to an application. The selection guide is divided into variables pertaining to the ion beam source, it grids, the beam, target, substrate, and deposition environment.

Table 4. Ion Beam Source Variables.

VARIABLE	GUIDELINE
Additional source, or *Assist Beam*	The addition of a second ion beam, also called an *assist beam*, is used for ion beam assisted deposition (IBAD). The assist beam is directed at the substrate and used for material modification. The modifications include promotion of oxidation, index of refraction control, and film stress reduction [15-17]. The assist beam can also be used for substrate pre-cleaning (or etching) to promote adhesion.
Source Type	RF for deposition of oxides (process that require oxygen); production runs. DC hollow cathode for deposition of metals; production runs. DC filament cathode for research and development; short runs.
Ion Specie	Argon for sputtering applications. Mixtures of Ar and O_2 are useful for reactive sputtering, however deposition rate (D_r) will decrease. For nitride formation, N_2 and CH_4 or C_2H_2 can be used for diamond like carbon (DLC) formation [18].
Flow Rate	Will be dependent upon source size and pumping speed of vacuum system. Typical flow is about 5 sccm Ar for 3 cm source. Typical flow is about 20 sccm Ar for 16 cm source. Maximum background pressure is about $5x10^{-4}$ mbar.

Table 5. Ion Beam Grid Variables.

VARIABLE	GUIDELINE
Grid Material	Molybdenum grids are dished to form convergent beams (sputtering applications) or divergent beams (assist applications). Molybdenum grids are preferred for processes that require oxygen (deposition of oxides). Graphite grids are flat and are used in processes that do not use oxygen.
Grid Style	Convergent molybdenum grids have minimal overspray ideal for sputtering. Divergent molybdenum grids have optimum beam spread for assist applications. Flat graphite grids have a flat beam profile required for etching.
Grid Erosion	The accelerator grid is typically the first grid to erode under normal conditions. The grid life is determined by the background pressure and applied accelerator voltage. Molybdenum grid erosion is about 5000 hours and graphite grid erosion is about 10,000 hours.
Number of Grids	For sputtering applications 3 grids are recommended. The decelerator grid protects the accelerator grid from becoming coated. For dielectric materials, this protection stabilizes the beamlet trajectories and thus promotes a more stable deposition plume.
Grid Cleaning	For dielectric applications, cleaning should be performed frequently as film stress will mechanically distort the grid assembly. About every 200 hours is recommended. For metal coatings, the cleaning cycle will depend upon the rate of formation of metallic flakes on the grids which can produce electrical shorts. Between 500 to 1000 hours is recommended. Mechanical cleaning of molybdenum grids is accomplished by using a blast cabinet with Al_2O_3 media at low pressure.

Table 6. Beam Conditions.

VARIABLE	GUIDELINE
Ion Energy or Beam Voltage	For sputtering applications ion energies between 1000 to 1500 eV are typical. For assist applications, ion energies between 100 to 500 eV are typical.
Beam Current	The maximum beam current will determine the maximum deposition rate (D_r). The maximum beam current for an ion beam source depends upon the source size, grid and source design. However, a rough approximation is: $$\textit{Maximum beam current} = 3\ (mA/cm^2) \cdot A_{Beam} + 50\ mA,$$ where A_{Beam} is the area of the beam at source exit. For example, an 8 cm source will have a beam area of 50 cm^2 and a maximum beam current of about 200 mA. Assist applications require low beam current.
Accelerator Voltage	The accelerator voltage will determine the degree of beamlet collimation. For sputtering the voltage should be around -250 V (focused). For assist applications, the voltage can vary from -100 to -700 V.

Table 7. IBS Target Variables.

VARIABLE	GUIDELINE
Target angle	Angle between source centerline and target normal is typically 45° for sputtering applications. Maximum sputter yield (S_y) for some materials will be at angles between 60° and 75°.
Target material	Metal targets, such as Ta, Ti, Hf, with a nearby oxygen gas line can be used to produce oxides Ta_2O_5, TiO_2, HfO_2. It is also recommended to have a nearby oxygen line for ceramic targets, such as SiO_2, so the target does not become metal rich, or Si rich in the case for SiO_2.
Target motion	Oscillation of the target will promote even wear and reduce texturing. Texturing will induce drift in deposition rate and uniformity. Typical oscillation can be ± 4° from the set angle.
Target Life	The target life can be estimated by: $$\text{Life} = \frac{T}{E_r}\ \text{(min)},$$ Where T is target thickness in Å, and E_r is estimated from Equation 1.

Table 8. Substrate Variables.

VARIABLE	GUIDELINE
Cleanliness	For good adhesion, substrates must be properly cleaned. Oils and debris can be removed with solvents such as acetone and isopropyl alcohol. Substrates can be pre-cleaned using the assist beam which will etch the surface oxide layer.
Substrate Temperature	Steady-state substrate temperature is process and mount configuration dependent but is on the order of 100°C. For some materials, deposition rate (D_r) will decrease with substrate temperature as much as 0.3%/°C. Water cooled fixtures can be used to remove heat from the substrates.
Thickness	Oxide films will have high compressive stress on order of 500 MPa. The degree of substrate distortion decreases with substrate thickness increase.

Table 9. Deposition Environmental Variables.

VARIABLE	GUIDELINE
Background Pressure	The general rule is the lower the background pressure the higher the quality of coatings. Higher background pressure will give rise to gas entrapment in the deposited film and lower deposition rate (D_r). At pressures above $1x10^{-3}$ mbar the ion beam source may ignite an uncontrolled discharge around its electrical connections and will have unstable operation.
Contamination	If the ion beam is not focused on the target, beam overspray will induce contamination in the deposited film. Other causes of contamination include material from the erosion of accelerator grid and filament (DC source).
Target Oxygen Flow Rate	The production of oxides will require a gas line near the target. The flow rate is optimized when the optical loss for the film is minimized. Actual flow rates are process dependent, however, they are on the order of 20 sccm.

Final Comments

This article provides a brief introduction into ion beam sputtering. A description of standard ion beam sputtering systems (IBS) and ion beam assisted (IBAD) are presented. Sputter yield and etch rate are discussed. Finally, key parameters are identified and tabulated for reference.

References

[1] Wilbur P J, Rawlin V K, and Beattie J R, 1998 Ion Thruster Development Trends and Status in the United States *J. Prop. and Power*, V. 14, No. 5, pp. 708-715.

[2] Kaufman H R and Robinson R S, 1990 Broad-Beam Ion Sources in *Handbook of Plasma Processing Technology*, pp. 183-193.

[3] Forster J C and Keller J H 1995 Planar Inductive Sources in *High Density Plasma Sources*, pp. 76-99.

[4] Kaufman H R and Robinson R S 1984 *Operation of Broad-Beam Sources*, pp. 34-47, Commonwealth Scientific Co, Alexandria, VA.

[5] Monheiser J M, Wilbur P J, 1992 An Experimental Study of Impingement-Ion-Production Mechanisms *28th Joint Propulsion Conference*, AIAA Paper 92-3826.

[6] Kaufman H R and Robinson R S 1984 *Operation of Broad-Beam Sources*, pp. 14, 49-51, Commonwealth Scientific Co, Alexandria, VA.

[7] Mahan J 2000 *Physical Vapor Deposition of Thin Films* pp. 199-264.

[8] Ruzic D N 1990 Fundamentals of Sputtering and Reflection in *Handbook of Plasma Processing Technology*, pp. 70-90.

[9] Kaminsky M 1965 *Atomic and Ionic Impact Phenomena on Metal Surfaces* pp. 142-232.

[10] Rosenberg D and Wehner G K 1962 Sputtering Yields for Low Energy He^+, Kr^+, and Xe^+ Ion Bombardment *Journal of Applied Physics* Vol. 33(5), pp. 1842-1845.

[11] Ziegler J F and Biersack J P, *SRIM 2003* (Program and Documentation) www.srim.org (2009)

[12] Williams J D, Gardner M M, Johnson M L and Wilbur P J 2003 Xenon Sputter Yield Measurements for Ion Thruster Materials *28th Int'l Electric Propulsion Conf*. paper IEPC-03-130.

[13] Macleod A H 2001 *Thin Film Optical Filters* pp. 257-345 (Institute of Physics Publishing)

[14] Poitras D, Cassidy T and Guetre S 2001 Asymmetrical Dual-Cavity Filters: Theory and Application *Proceedings, Optical Society of America, OIC Conference*.

[15] McNally J J 1990 Ion Assisted Deposition in *Handbook of Plasma Processing Technology* pp. 466-482.

[16] Wu Y C, Wu J Y and Lee C C 2004 The Effect of Assisted Ion Beam to Ta_2O_5 in a Dual Ion Beam Sputtering *Optics and Photonics Conf.*, paper PE-SA-30.

[17] Blair D G et. al 1997 Development of Low-Loss Sapphire Mirrors *Applied Optics* V. 36, No. 1, pp. 337-341.

[18] Wilbur P J and Buchholtz B W 1994 Surface Engineering using Ion Thruster Technology *30th Joint Propulsion Conference* AIAA Paper 94-3235.